



BNL-101758-2014-TECH

RHIC/AP/103;BNL-101758-2013-IR

The Conceptual Design of the RHIC92 Insertion

S. Tepikian

June 1992

Collider Accelerator Department
Brookhaven National Laboratory

U.S. Department of Energy

USDOE Office of Science (SC)

Notice: This technical note has been authored by employees of Brookhaven Science Associates, LLC under Contract No. DE-AC02-76CH00016 with the U.S. Department of Energy. The publisher by accepting the technical note for publication acknowledges that the United States Government retains a non-exclusive, paid-up, irrevocable, world-wide license to publish or reproduce the published form of this technical note, or allow others to do so, for United States Government purposes.

DISCLAIMER

This report was prepared as an account of work sponsored by an agency of the United States Government. Neither the United States Government nor any agency thereof, nor any of their employees, nor any of their contractors, subcontractors, or their employees, makes any warranty, express or implied, or assumes any legal liability or responsibility for the accuracy, completeness, or any third party's use or the results of such use of any information, apparatus, product, or process disclosed, or represents that its use would not infringe privately owned rights. Reference herein to any specific commercial product, process, or service by trade name, trademark, manufacturer, or otherwise, does not necessarily constitute or imply its endorsement, recommendation, or favoring by the United States Government or any agency thereof or its contractors or subcontractors. The views and opinions of authors expressed herein do not necessarily state or reflect those of the United States Government or any agency thereof.

AD/RHIC/AP-103

RHIC PROJECT
Brookhaven National Laboratory

The Conceptual Design of the RHIC 92 Insertion

S. Tepikian, M. Harrison

June 1992

The Conceptual Design of the RHIC 92 Insertions

S. Tepikian, M. Harrison

March 1992

Abstract

An upgraded version of the RHIC 91 insertion design is proposed that addresses many of the recommendations made at the August, 1991 Lattice Review Committee¹. The RHIC 92 lattice retains the anti-symmetric quadrupole arrangement in the interactive regions (IR), the long contiguous drift spaces and the same arcs of the RHIC 91 lattice. The quadrupole triplet and crossing dipoles have been modified in order that the D0(BC2) dipole can have a 10 cm aperture, giving a potential increase in the dynamic aperture. Furthermore, an intuitive approach was used to deal separately with the twiss functions (i.e., α_x , α_y , β_x and β_y) and the dispersion (i.e., η_x and η'_x). The new lattice has a larger tuning range in β^* than RHIC 91. Additionally, the lattice has been tuned to 7 different operating points (as of this writing).

Introduction

In August, 1991, a Lattice Review Committee¹ was set up to evaluate the RHIC 91 lattice² and two other potential RHIC lattices: RHICAGR³ and RHICJC⁴. The committee introduced two sets of criteria to evaluate the lattice designs presented. The criteria are quoted below:

Class A: criteria that are most important and must be met.

- A1. β^* flexibility
- A2. Long and contiguous warm space
- A3. Abort away from IP (interaction point)
- A4. No requirement for precise matching
- A5. Flexibility of matching
- A6. Compatability with a Mini- β^* option

and

Class B: criteria that are desirable and should be pursued

- B1. Modular dispersion suppressor
- B2. Parallel beam lines after Q3
- B3. Compact IR triplets
- B4. Capacity of $\Delta\Phi$ (IP to IP) $\approx 90^\circ$

The committee concluded “that they [RHIC 91, RHICAGR and RHICJC] do not, as presented, meet all of Class A, and are therefore not recommended as is.”

A lattice is proposed, denoted RHIC92, that meets all the criteria in Class A and most of the Class B criteria. Additionally, the poor dynamic aperture of the RHIC91 lattice was addressed. A modified triplet design that potentially enhances the dynamic aperture was found.

The design of the RHIC92 lattice is presented in the following sections.

Insertion Components

In general, an insertion can be characterized with two main components as shown in Fig. 1.: (1) the telescope which reduces the beam size at the IP to enhance the luminosity when colliding the two beams and (2) the matching section which matches the telescope to the arcs so that all the insertions can be treated independently, at least to first order (in RHICAGR and RHICJC, the matching section is also a dispersion suppressor).

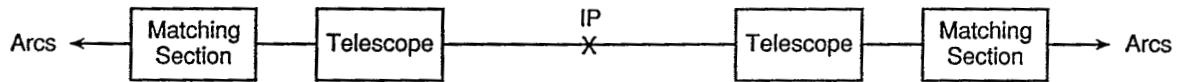


Fig. 1 A schematic of an insertion.

The elements that make up the matching section and telescope are quadrupoles, dipoles and drift spaces. A telescope (shown in Fig. 2) is composed of two groups of quadrupoles: a triplet (Q1, Q2 and Q3), generally with a long focal length, placed as close to the IP as possible (which is analogous to the objective lens of a telescope) and a douplet (Q4 and Q5) near the matching section (which is analogous to the eyepiece or ocular of a telescope). Alternative configurations to this telescope also exist. Furthermore, dipoles may be required to bring the beams together at the IP.

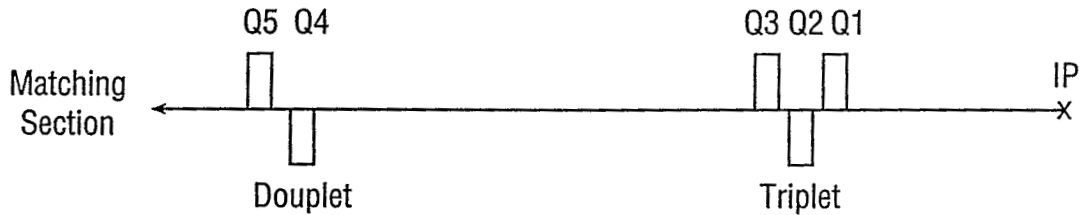


Fig. 2 A telescope.

In RHIC, two dipoles in the telescope are used to bring the beams together. The dipole closest to IP is common between the two rings, see Fig. 3.

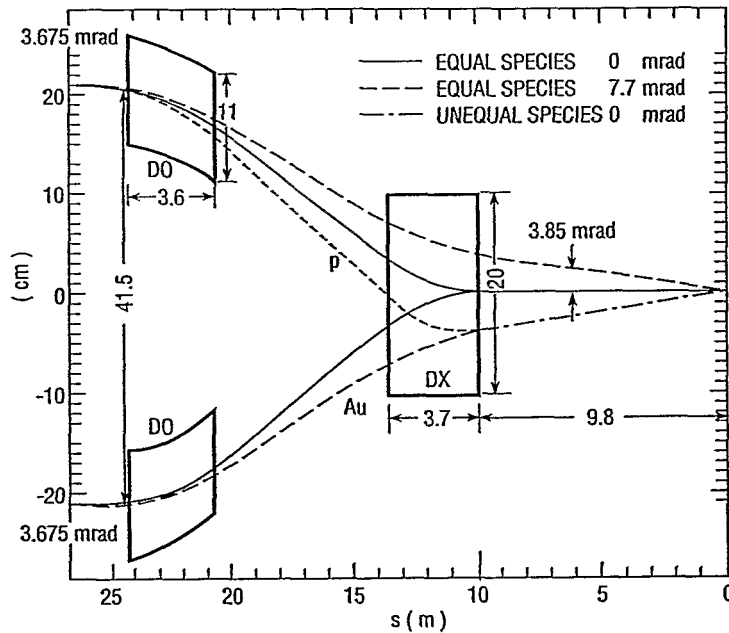


Fig. 3 The crossing point dipoles.

RHIC is required to be able to collide beams of different species, such as protons against gold. These two species bend differently in the common dipole DX (the proton bend angle is 2-1/2 times the bend angle of gold). In order for the beams to collide head on, D0 and DX must be adjusted such that both beams cross the central axis with a non-zero angle, α , as in Fig. 3. Appendix I shows how to calculate the curvature of the D0 and the DX magnets.

Since the beam orbit changes between D0 and IP as the particle species is changed, it becomes impractical to place the telescope's quadrupole triplet anywhere between IP and the D0 magnet. Furthermore, the triplet and D0 magnets must be placed as close to the IP as possible in order to reduce the corresponding β functions. Particle tracking studies in RHIC91 have shown that the D0 magnet is the limiting factor in the dynamic aperture^{5, 6}. In light of these results, the following changes were made to the triplet and D0 magnets in RHIC92: (1) the triplet was compacted in order to reduce the β_{\max} , (2) D0 (and the associated triplet) were moved 1.4m further from DX so that the coil aperture of D0 can be increased from 8 cm diameter to 11 cm and (3) the sizes of the triplet quads were normalized to a field of 47.6 T/m (at top energy) to reduce shunt supply requirements. From the above list, item (1) reduces the β 's in the triplet, however, items (2) and (3) increase the β functions in both the triplet and D0. The final tally for RHIC92 leads to

β_{\max} 's that are 6% larger in the triplets and β 's that are 12% larger in D0. The increase in beta values in the triplet were thus involved in a trade-off with the increase in aperture of the D0 magnet. The arrangement chosen provides an approximate matching between the aperture in these two elements.

Additionally, in order to keep D0 as close as possible to DX, the two beams are separated at 41.5 cm at D0. The beams diverge at a small angle (3.675 mrad) until they reach 90 cm separation at D5. The beams remain separated at 90 cm till the next insertion. The detailed geometry of dipole D5 is described in Appendix II.

Finally, the remaining magnets of the insertion form the matching section. This section is composed of two complete FODO cells. Unlike RHIC91, the drift space lengths between the quadrupoles are kept equal (except for dipoles, where perturbing these lengths is required for geometric reasons).

Symmetry of the Insertion

The previous section only discussed the matching section and telescope on the left side of the IP. The insertion components on the right side of the IP is to have the twiss parameters and dispersion either symmetrically or anti-symmetrically related to their corresponding functions on the left side. Thus, we have a choice of four possibilities: either the dipoles (D0 and DX) are symmetric or antisymmetric across the IP and the quadrupoles are symmetric or anti-symmetric across the IP. Note that except for dipoles DX, D0 and D5, all dipoles will be symmetric across the IP.

In order to allow colliding beams of different species, dipoles D0 and DX must be anti-symmetric across the IP. Furthermore, the inner arcs and outer arcs are different lengths. With an anti-symmetric dipole arrangement, the beam spends half its time in the inner arcs and the rest of the time in the outer arcs, equalizing this difference.

With the anti-symmetric dipole arrangement and the requirement of zero dispersion, η , at the IP (i.e., to minimize the beam size at the IP), the η is anti-symmetric and the η' is symmetric about the IP. When the dispersion is antisymmetric, a symmetric quadrupole arrangement will preserve symmetries of η and η' . This can be seen from the thin lens model shown in Fig. 4. Note, that for an anti-symmetric quadrupole arrangement, the symmetries are broken. Thus, it is natural to use a symmetric quadrupole arrangement about the IP. RHICAGR and RHICJC used this approach, which simplifies the lattice by using dispersion suppressors for the matching sections.

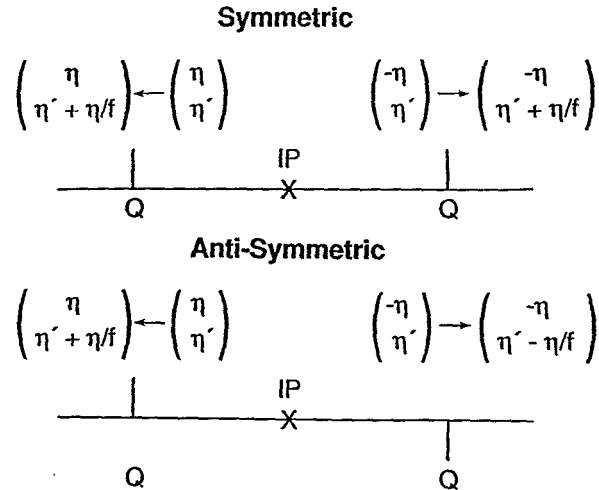


Fig. 4 A thin lens kick to dispersion where f is the focal length of quadrupole Q .

The symmetric quadrupole arrangement, however, leads to large chromaticities since the contributions to the chromaticity add rather than cancel. Such a lattice will require large sextupoles to correct the chromaticities increasing the non-linearities in the machine. Furthermore, more than two families of sextupoles will be required to obtain a minimum tune variation with momentum. Additionally, a solution could not be found with a large warm drift space.

In choosing an anti-symmetric quadrupole arrangement about the IP, the contributions to chromaticity cancels about the IP. For this reason RHIC92 adopted the anti-symmetric quadrupole arrangement. Note, RHIC92's chromatic behaviors⁶ are superior to both RHIC91 and RHICAGR. Additional advantages of the anti-symmetric lattice are: (1) the lattice is tunable to $\beta^* = 1$ m with a large warm drift space present and (2) a mini- β^* option is available. These two advantages are part of the Class A criteria from the Lattice Review Committee.

With the adoption of an anti-symmetric quadrupole arrangement, the insertion design is a little more involved. Figure 4 shows that the symmetry of η' is not preserved in the antisymmetric lattice. In the SSC, a group of cells with a -1 transfer function are used between the two dipoles and dispersion suppressors are used for the matching sections.⁷ This design cannot be implemented in RHIC for two reasons: (1) the presence of quadrupoles between D0 and IP prevent the colliding of unequal species and (2) there is not enough space available in RHIC. In the following section, a design for the RHIC lattice is presented that deals intuitively with the dispersion.

Tuning the Twiss Functions

First choose a β^* where most of the experiments are expected to be performed.

For RHIC, $\beta^*=2m$ was chosen. Second, put the insertion together from the components described in the previous two sections. Then our goal is to find the required quadrupole strengths to achieve the $\beta^*=2m$ at the IP and match the insertion to the arcs. For this exercise, dispersion is ignored.

To be more specific at the IP choose $\beta_x(\text{IP}) = \beta_y(\text{IP}) = \beta^*$. Furthermore, in order to have the β functions anti-symmetric across the IP, it is necessary that $\alpha_x(\text{IP}) = \alpha_y(\text{IP}) = 0$. Since the β_{max} in the triplets can be quite large, $\beta_{x(max)} = \beta_{y(max)} = \beta_{max}$ is imposed. At $\beta^*=2m$, then $\beta_{max} < 670m$ in RHIC92. Additionally, the gradients in QF and QD of the arcs are adjusted in order to obtain the nominal machine tunes of $\nu_x = 28.827$ and $\nu_y = 28.823$. Using the 7 conditions stated above (which assumes perfect anti-symmetry), a preliminary solution for the quadrupole strengths can be found which will be successively refined.

The anti-symmetry is broken, since, the inner arcs and outer arcs differ in length for geometric reasons breaking the anti-symmetry by about 2.4×10^{-3} units and the edge focussing of dipole DX (all other dipoles are assumed to be curved). The effect of the anti-symmetry breaking is reduced an order of magnitude by including two additional quadrupoles (7 quadrupoles) when tuning the twiss functions. The anti-symmetry breaking results in 4 additional conditions.

Finally, the best solution is found by combining the arcs and the insertions in a complete superperiod, and fitting the 7 quadrupoles and QF and QD to obtain 4 crossing point conditions, β_{max} condition, minimum, $\Delta\beta/\beta$ in the arcs and the proper operating tunes.

Tuning the Dispersion Functions

Once the Twiss functions are tuned, then we can tune the dispersion functions. The dispersion is tuned by adjusting the dipoles in the matching section. Since this has negligible effect on the Twiss functions, both sets of functions are tuned independently.

To minimize the beam size at the IP, set $\eta(\text{IP})=0$. Furthermore, the dispersion is anti-symmetric about the IP and can become quite large at the triplets, thus, $\eta'(\text{IP})$ must be kept small. Two additional conditions in an anti-symmetric lattice is matching the η and η' at the arcs.

These four conditions can be handled with four consecutive dipoles in two full cells making up the matching section. However, in RHIC, there are several constraints that can conflict with the ideal solution: (1) leaving room for septum and kicker magnets for injection, (2) minimizing the number of dipole types and (3) fitting the accelerator in the existing tunnel.

A solution was found (Fig. 5) which satisfied all three of the constraints listed above and three of the conditions on dispersion functions. In this solution, $\eta'(\text{IP})$ remained small and did not need special attention.

Tuning the insertion at other β^* s

When the insertion is tuned to different β^* s, only the quadrupole strengths will be changed. Since this will be done with the beam in the machine, the functions of the quadrupole strengths versus β^* must be smooth and continuous.

Recalling from the previous two sections, the most important conditions are:

$$\beta^* = \beta_x(\text{IP}) = \beta_y(\text{IP})$$

$$0 = \alpha_x(\text{IP}) = \alpha_y(\text{IP})$$

$$\beta_x(\text{max}) = \beta_y(\text{max})$$

$$0 = \eta(\text{IP})$$

η and η' matched to the arcs

$$\nu_x = 28.827$$

$$\nu_y = 28.823$$

These 10 conditions requires at least 10 quadrupoles for tuning. RHIC92 uses 11 quadrupoles: 9 quadrupoles in the insertion and QF and QD.

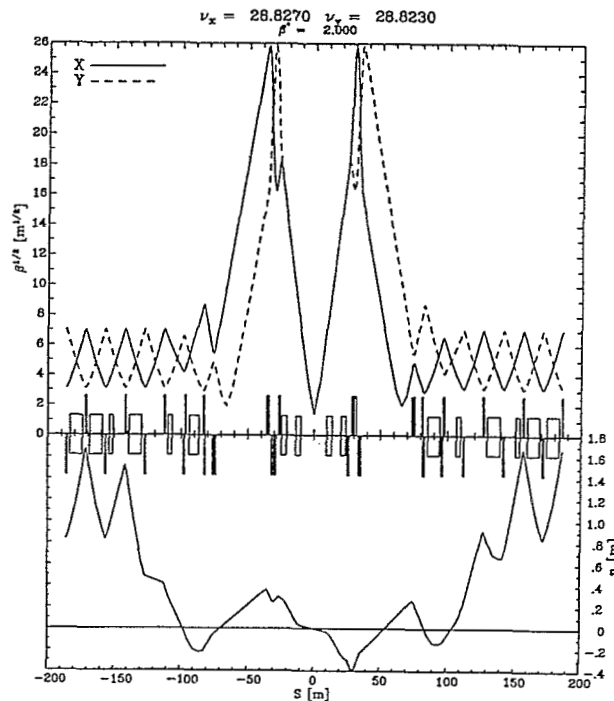


Fig. 5

RHIC92 has been tuned at the nominal operating points of $\nu_x = 28.827$ and $\nu_y = 28.823$ for $\beta^* = 0.5\text{m}$ to 200m . Beyond $\beta^* = 10\text{m}$ the β_{max} condition is turned off. Figures 6 and 7 show the tuning curves of the β^* versus quadrupole strengths for $\beta^* = 1\text{m}$ to 10m (the planned range in β^* for RHIC92 operation). Figures 8–12 shows the lattice functions of the insertion for $\beta^* = 0.5, 1, 6, 10$ and 200m respectively. An alternative tuning scheme is to keep QF and QD fixed which in turn keeps the phase advance across the insertion fixed. This is possible in RHIC92 for $\beta^* \leq 6\text{m}$.

The lattice has been tuned to 6 other operating tunes and corresponding figures listed in Table I.

Table I

ν_x	ν_y	Tuning Curves
28.557	28.553	Figs. 13–14
28.957	28.953	Figs. 15–16
28.197	28.193	Figs. 17–18
28.827	27.823	Figs. 19–20
29.197	28.193	Figs. 21–22
28.197	29.193	Figs. 23–24

This lattice was developed using the MAD version 8.17 program.⁸

Acknowledgements

We express our appreciation to A. Garren, E. Courant, S. Ohnuma, S.-Y. Lee, A. Ruggiero, J. Claus and the other members of the Lattice Review Committee for the many insightful discussions.

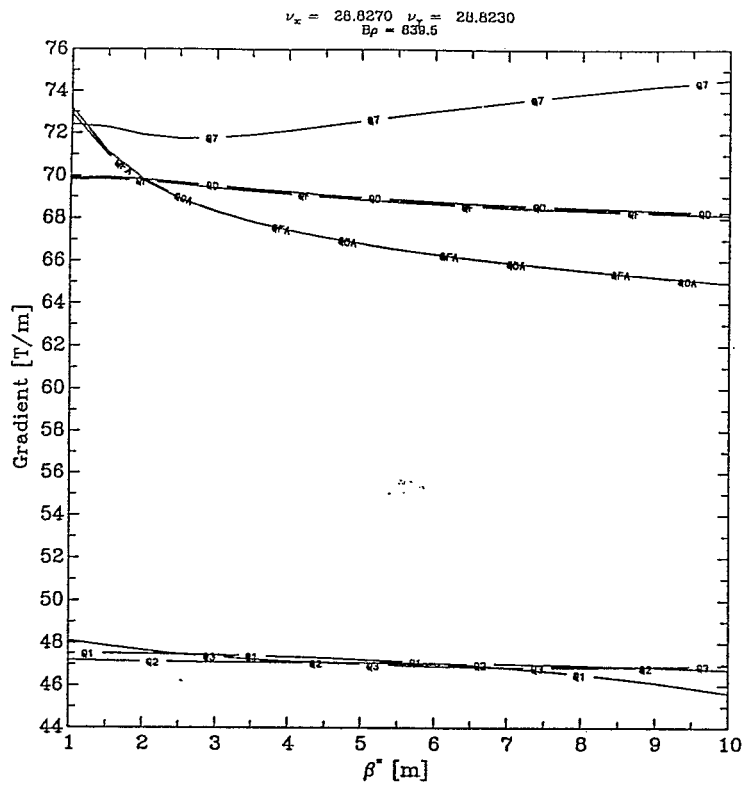


Fig. 6

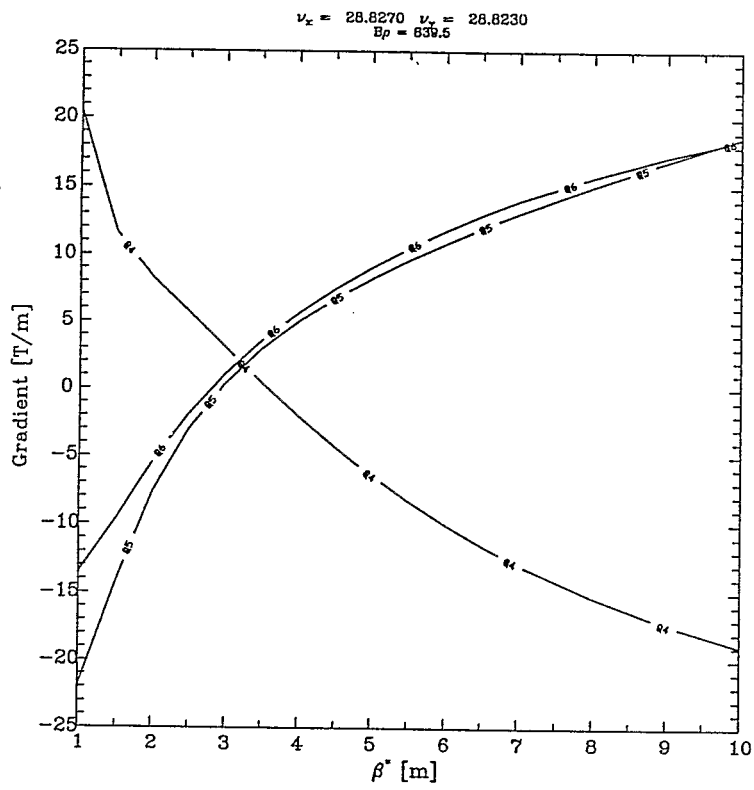


Fig. 7

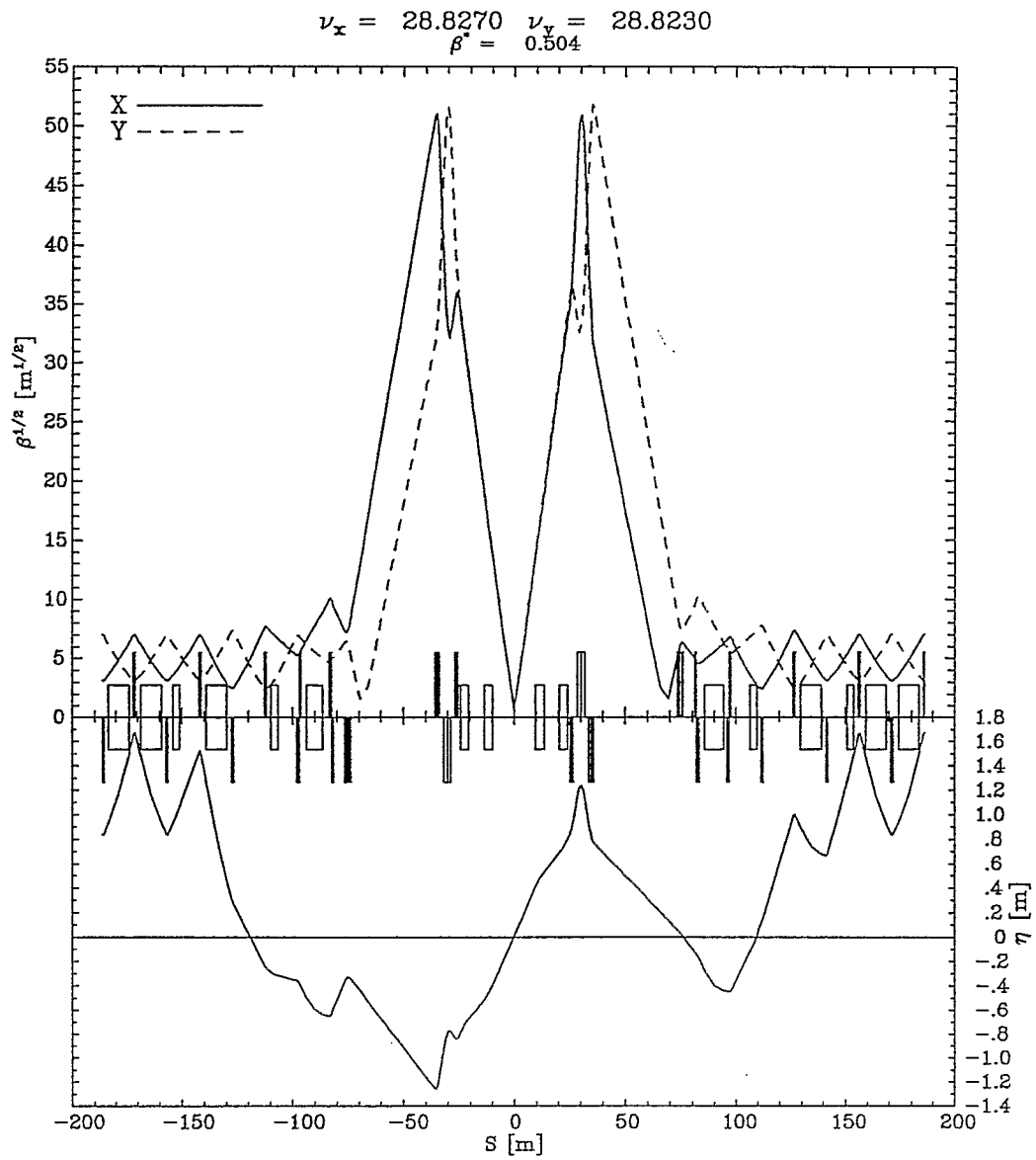


Fig. 8

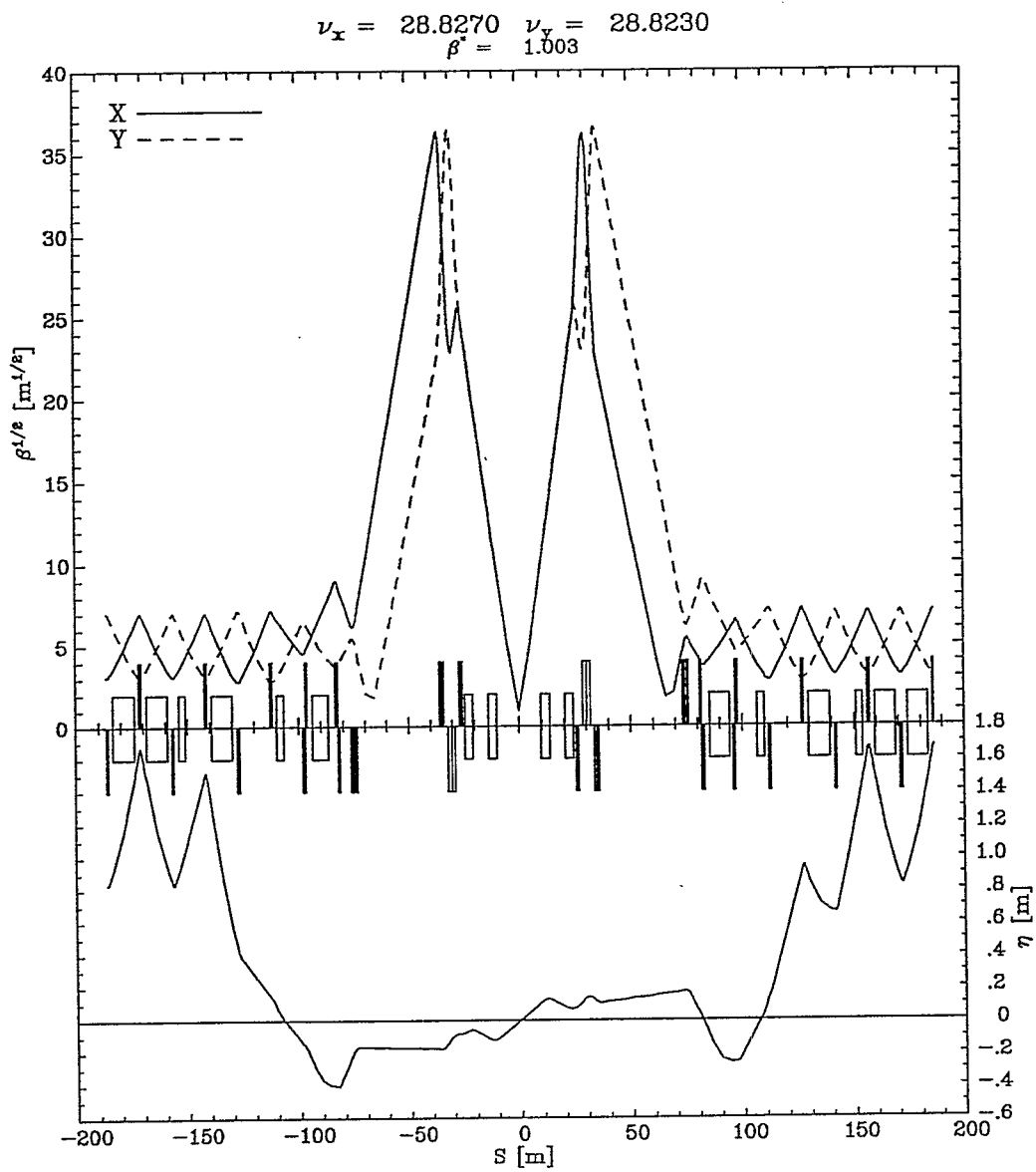


Fig. 9

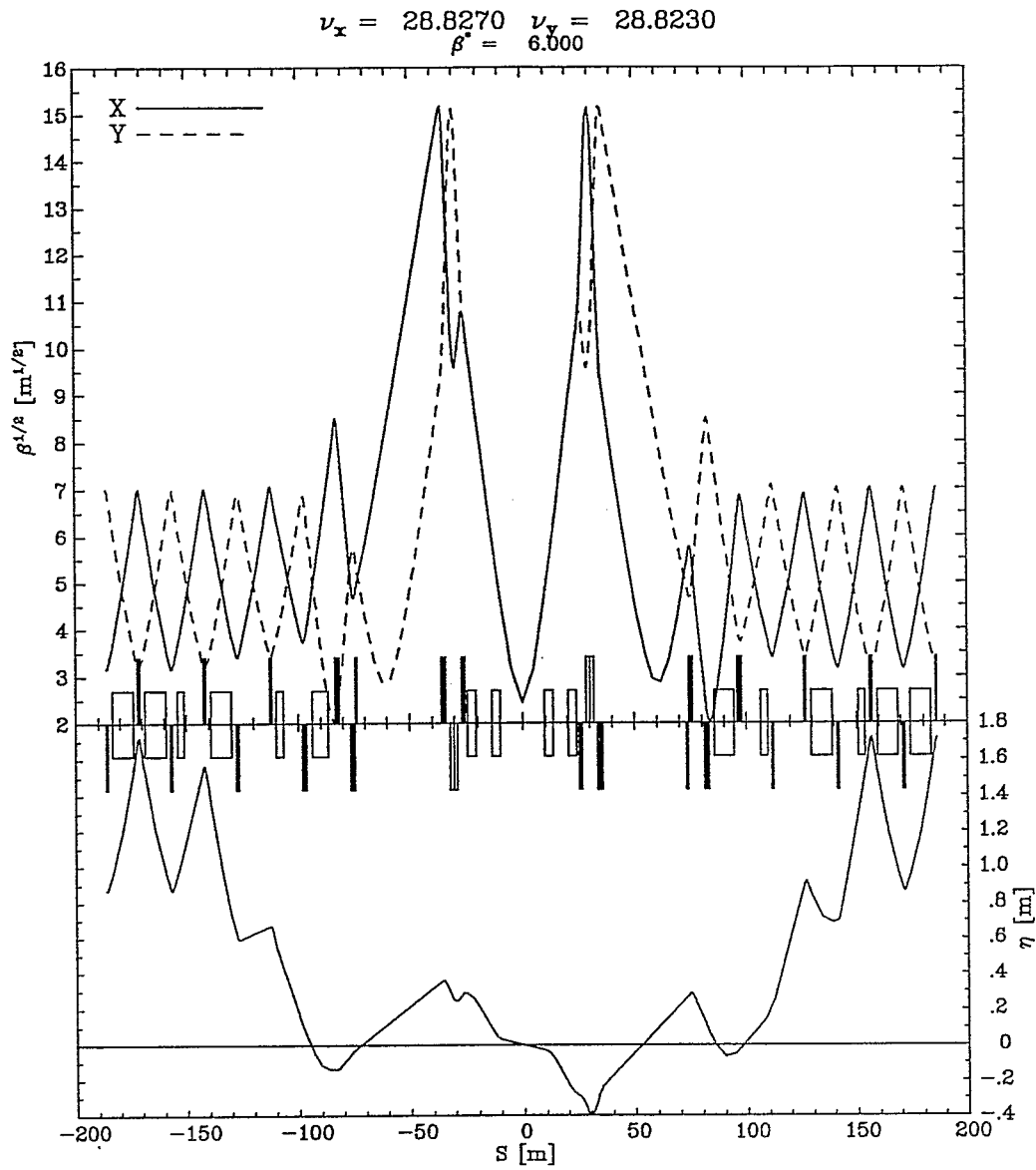


Fig. 10

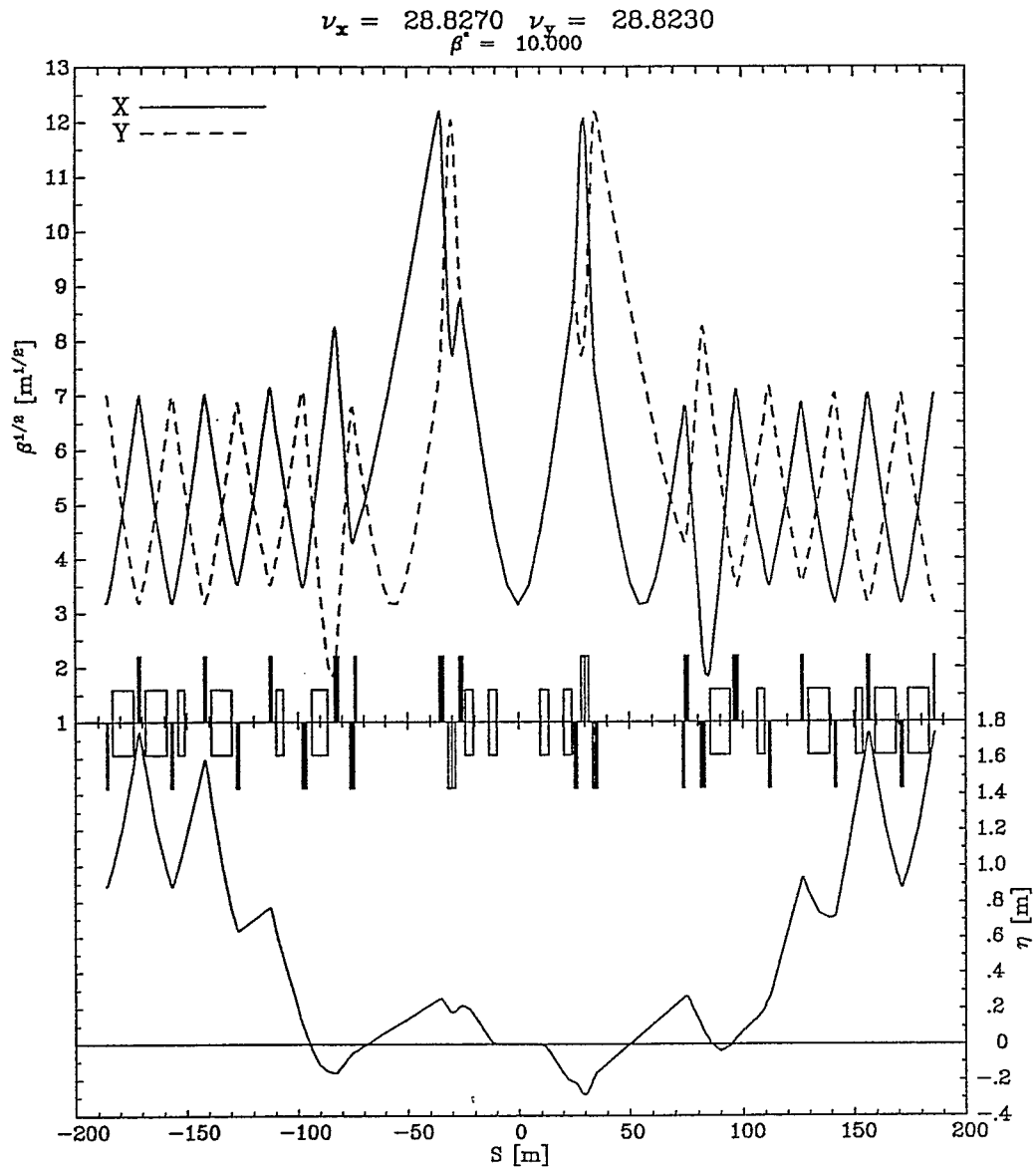


Fig. 11

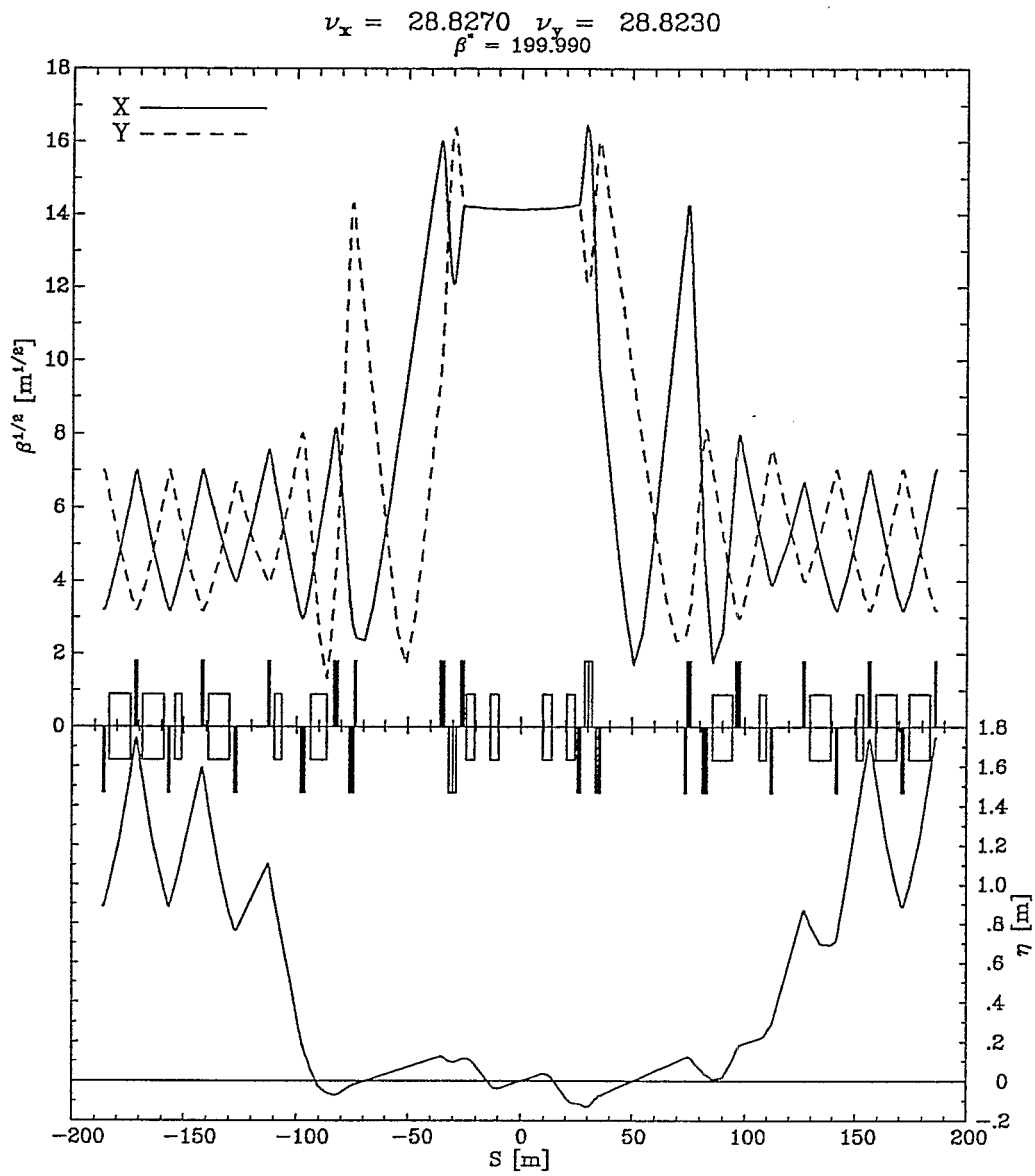


Fig. 12

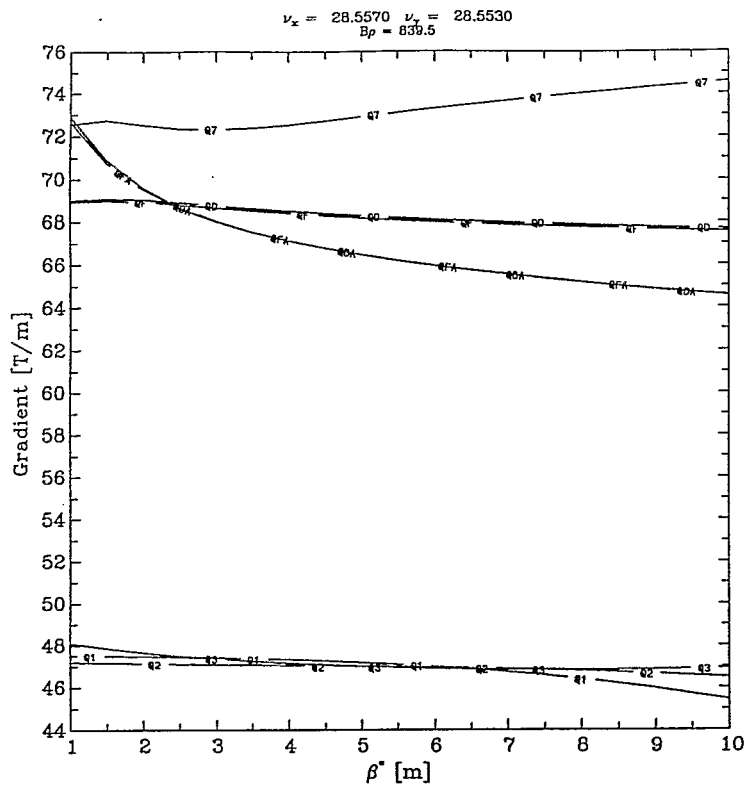


Fig. 13

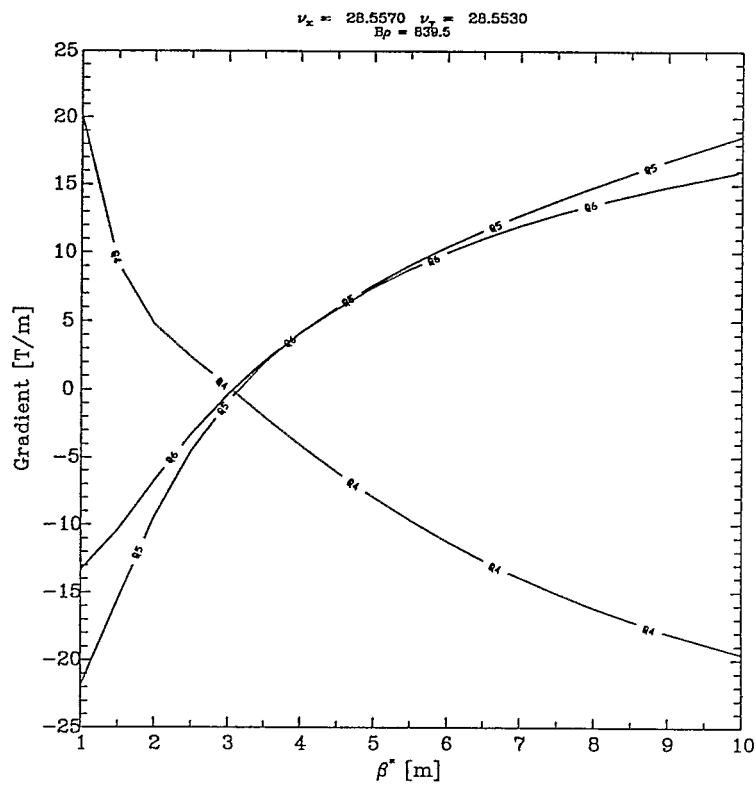


Fig. 14

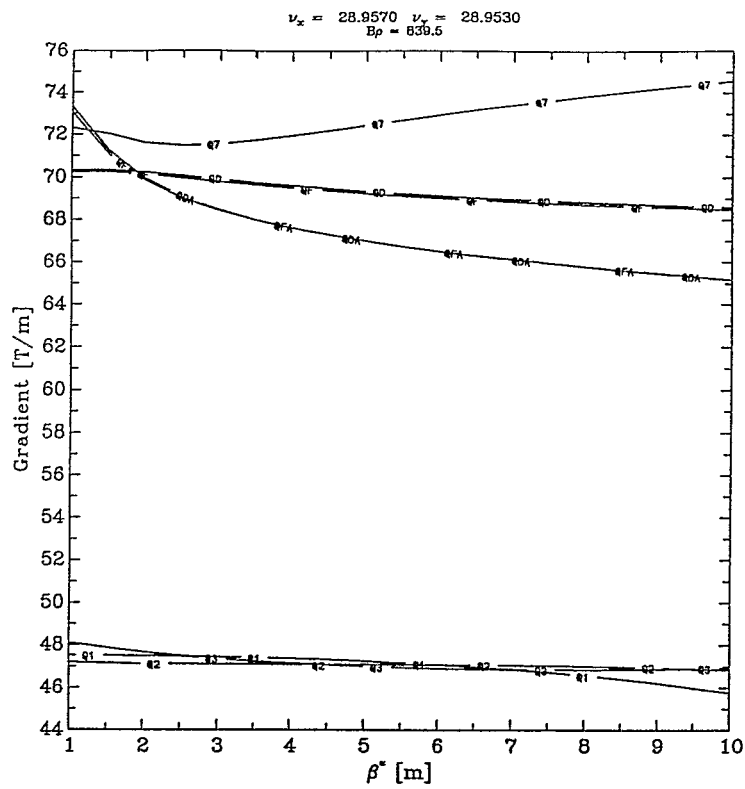


Fig. 15

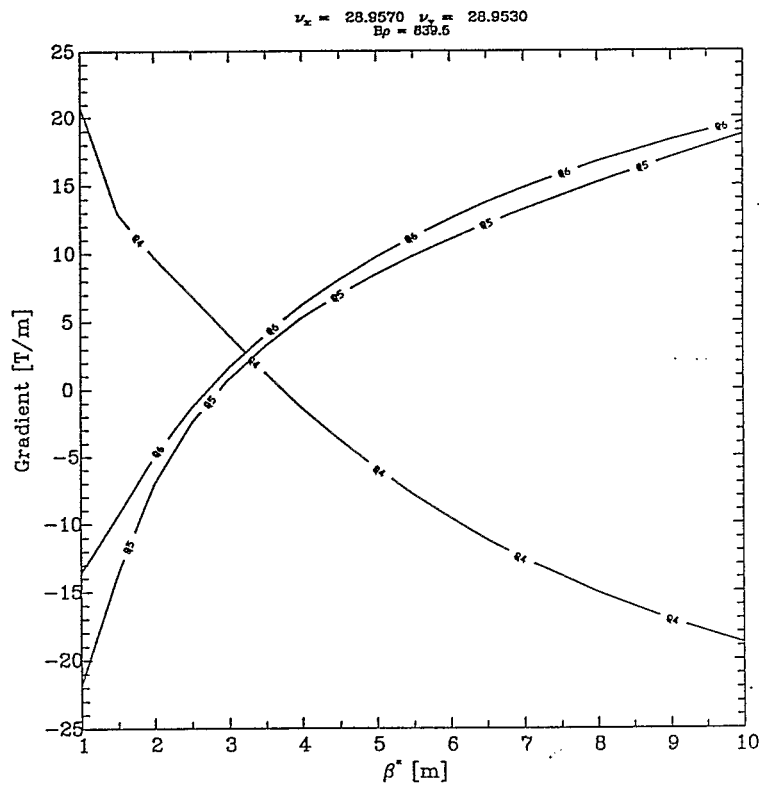


Fig. 16

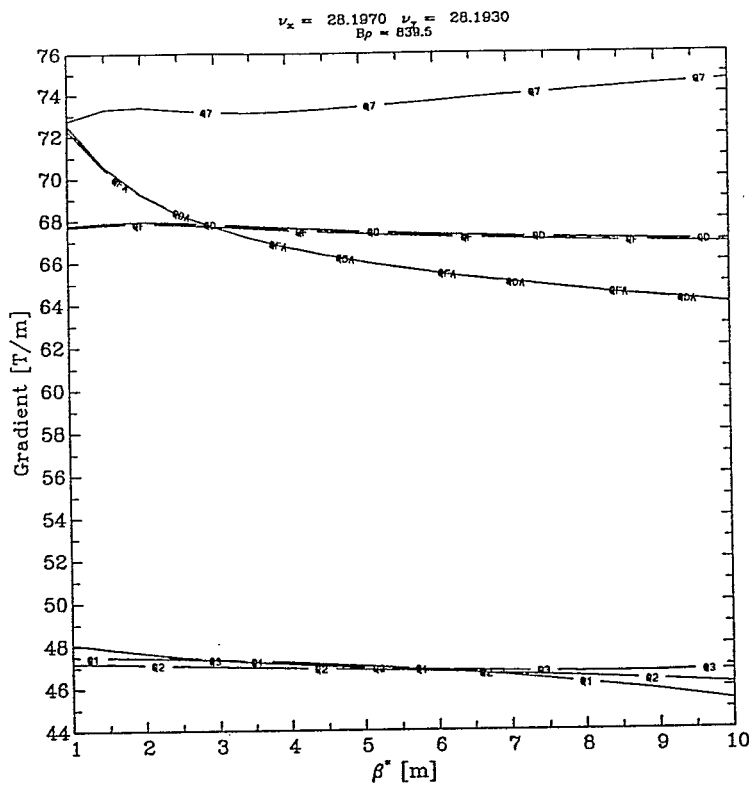


Fig. 17

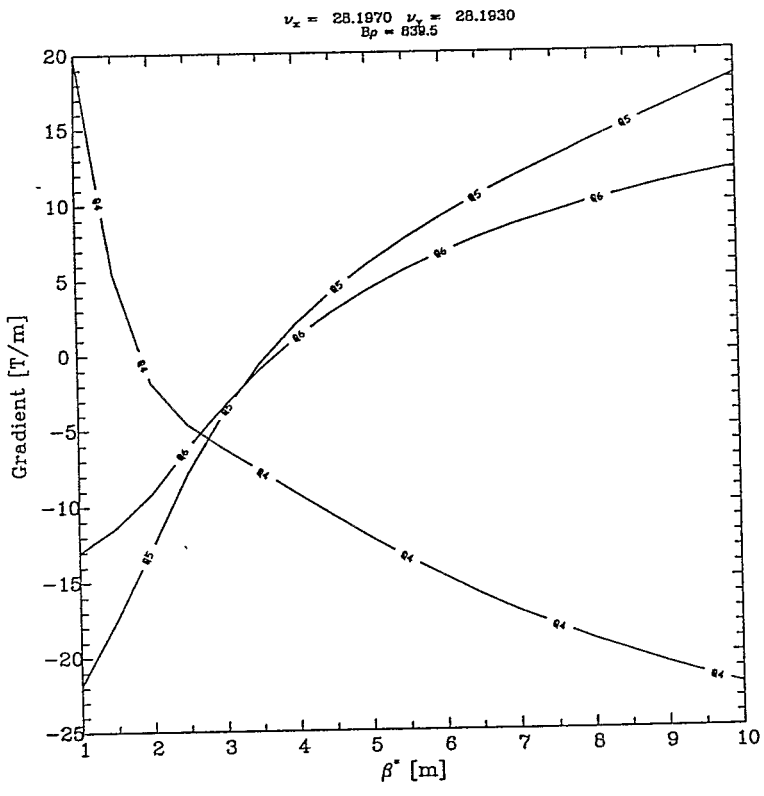


Fig. 18

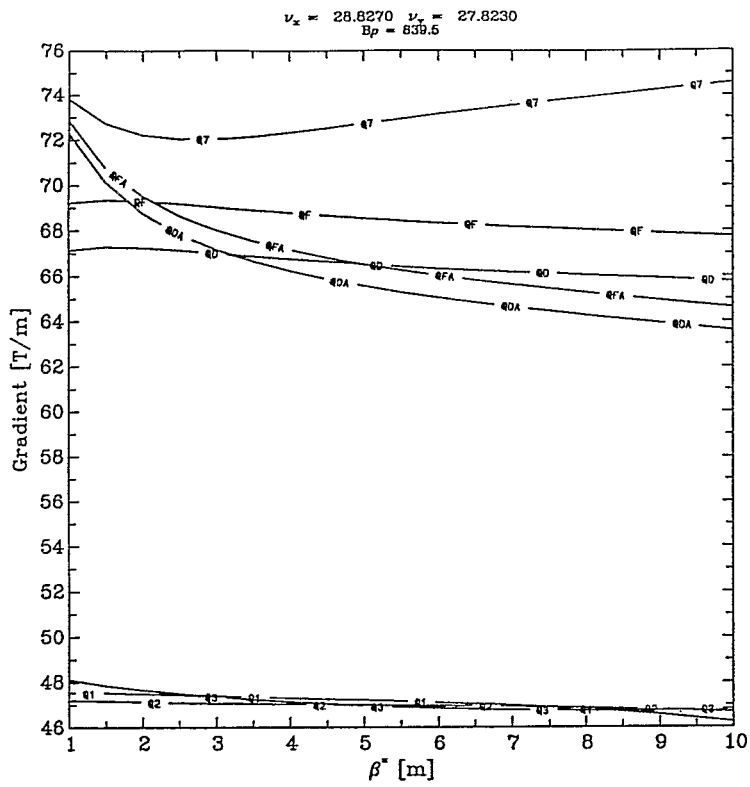


Fig. 19

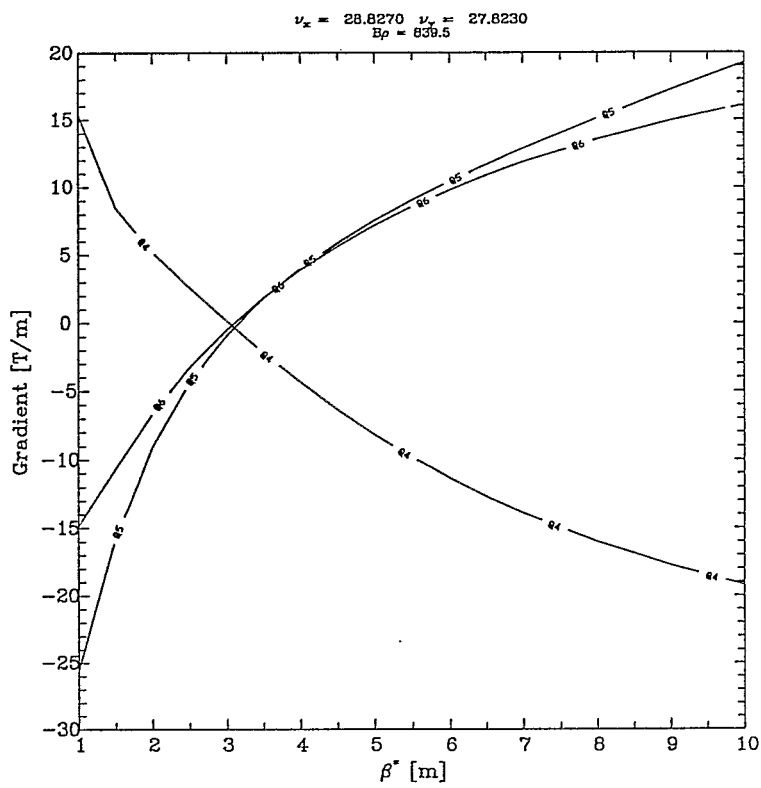


Fig. 20

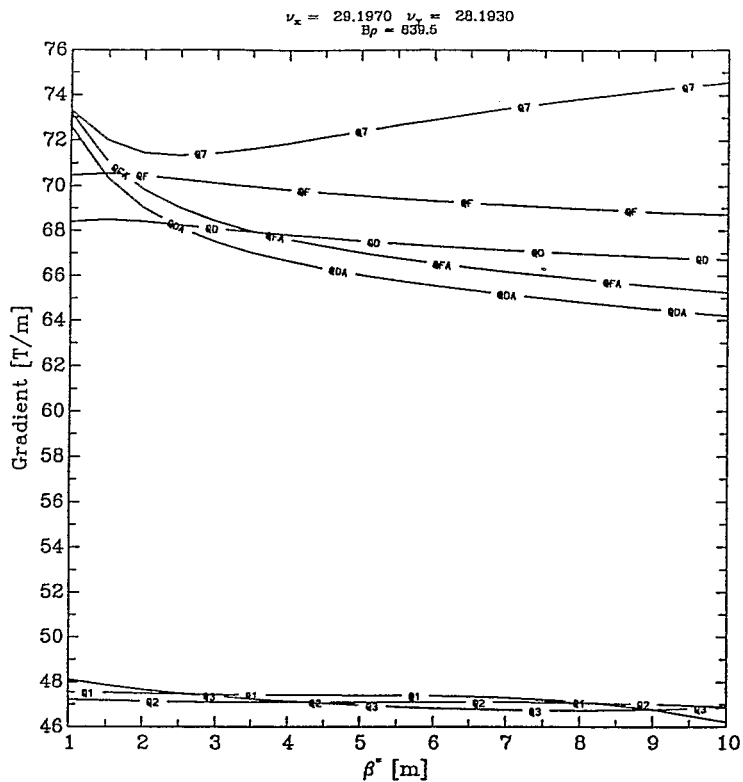


Fig. 21

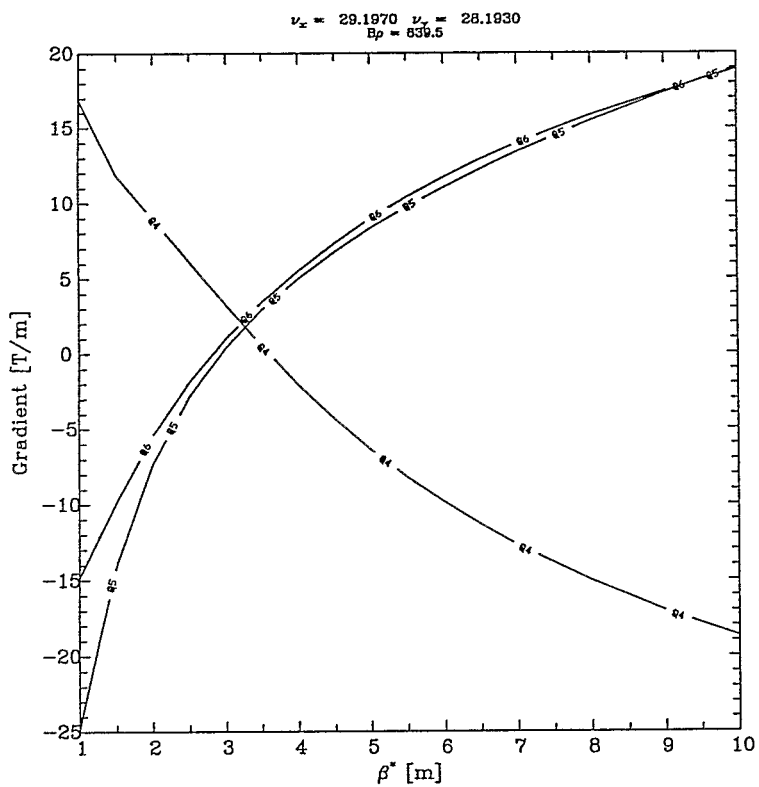


Fig. 22

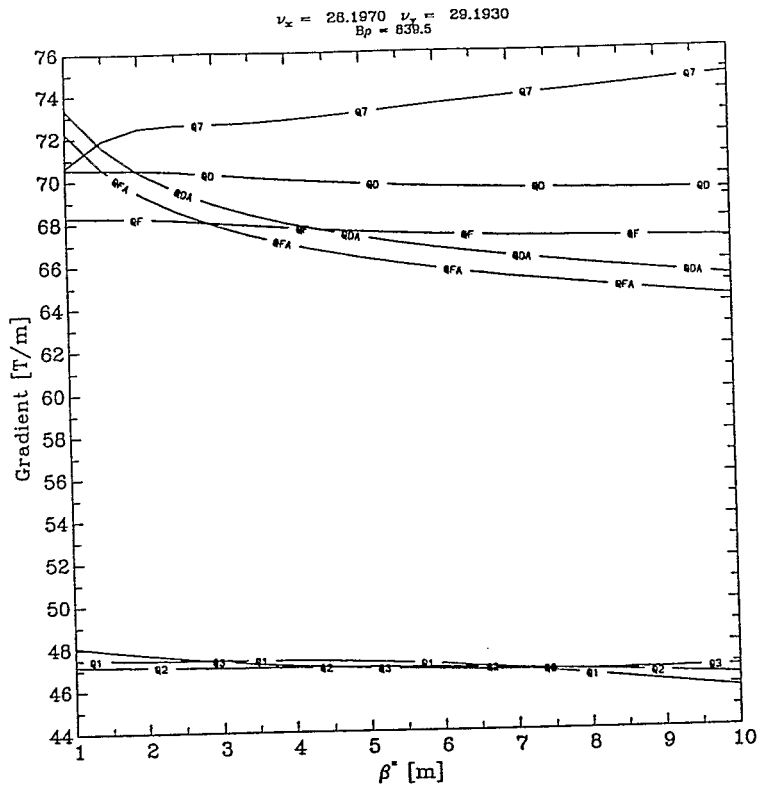


Fig. 23

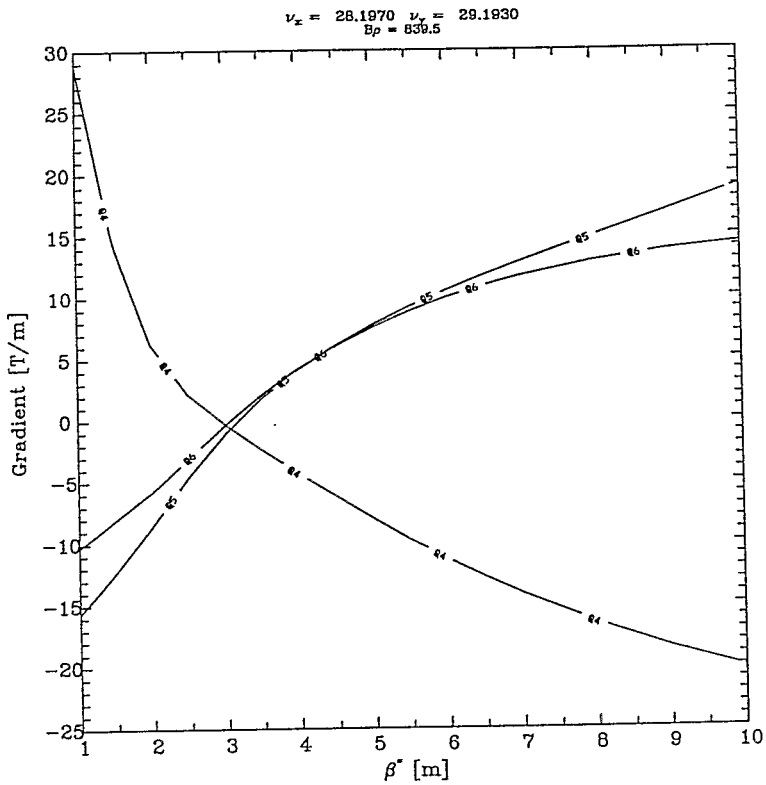


Fig. 24

References

1. A. Chao, "Report of the RHIC Lattice Review Committee", September, 1991.
2. S. Y. Lee, J. Claus, E.D. Courant, H. Hahn and G. Parzen, IEEE Nuclear Science, NS-32, 1626 (1985).
3. A.G. Ruggiero, "RHICAGR A Most Simplified RHIC Lattice", AD/AP-26 (1991).
4. J. Claus, private communication.
5. G. Parzen, private communication.
6. G.F. Dell, private communication.
7. A. Garren, private communication.
8. A. Grote and F.C. Iselin, "The MAD Program User's Reference Manual", CERN/SL/90-13(AP) (1990).

Appendix I.

The reference orbit through the dipoles D0 and DX must be adjusted to change the crossing angle of the beam. Since, the reference orbit doesn't go through D0 or DX symmetrically about the centers of the dipoles, these magnets cannot be handled in standard ways.

The reference orbit through the DX and D0 dipoles is shown in Fig. 25.

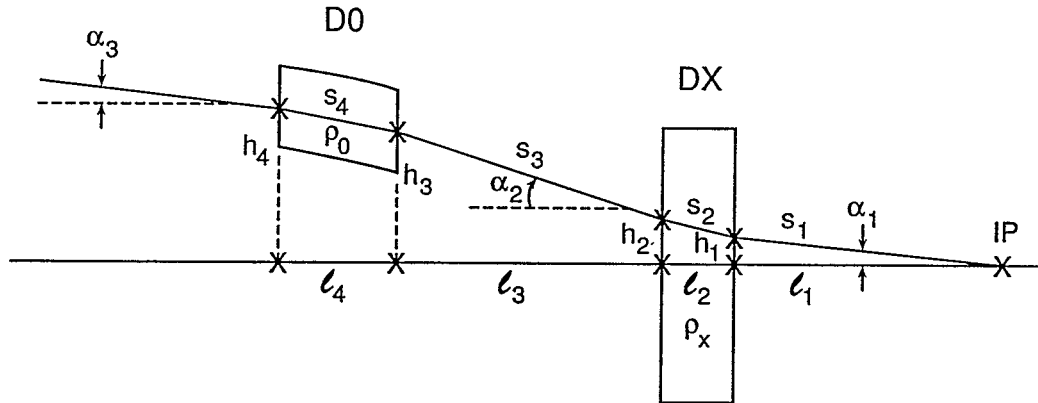


Fig. 25 Reference orbit through the crossing dipoles.

where l_1 , l_2 , l_3 and l_4 are the lengths of the dipoles and drift spaces as seen from a fixed coordinate axis, α_1 , α_2 and α_3 are the angles of the reference orbit relative to the fixed axis, h_1 , h_2 , h_3 and h_4 are the distances of the reference orbit from the fixed axis, s_1 , s_2 , s_3 and s_4 are the arc lengths of the reference orbit and ρ_0 and ρ_x are the radii of curvature for D0 and DX respectively.

In the drift space regions, the reference orbit remains along a straight line leaving

$$h_1 = l_1 \tan \alpha_1$$

$$s_1 = \frac{l_1}{\cos \alpha_1}$$

and

$$h_3 = h_2 + l_3 \tan \alpha_2$$

$$s_3 = \frac{l_3}{\cos \alpha_3}$$

In the dipoles, however, the path is along a curve with the radii ρ_0 and ρ_x . This curve can be deduced by solving the Lorentz force

$$m\gamma \frac{d}{dt} \mathbf{v} = q \frac{\mathbf{v}}{c} \times \mathbf{B}$$

in a fixed coordinate system. Integrating the Lorentz force leads to

$$h_2 = h_1 + l_2 \left[\sin\alpha_1 + \frac{l_2}{2\rho_x} \right]$$

$$\alpha_2 = \arcsin \left[\sin\alpha_1 + \frac{l_2}{\rho_x} \right]$$

$$s_2 = \rho_x (\alpha_2 - \alpha_1)$$

and

$$h_4 = h_3 + l_4 \left[\sin\alpha_2 - \frac{l_4}{2\rho_o} \right]$$

$$\alpha_3 = \arcsin \left[\sin\alpha_2 - \frac{l_4}{\rho_o} \right]$$

$$s_4 = \rho_o (\alpha_2 - \alpha_3)$$

With these system of equations, ρ_o and ρ_x are solved for to give the required angle, α_3 , and distance, h_4 , to match the reference orbit to the rest of the ring for any arbitrary crossing angle, α_1

Appendix II.

After the beams leave D0, the separation is less than 90 cm. The separation becomes 90 cm after dipoles D5I and D5O, after which the beams will be parallel. Fig. 26 shows the geometry in more detail.

From geometric considerations we have:

$$\tan\alpha = \frac{l_3 - l_1}{2l_2}$$

$$s_i = \frac{l_2 - \frac{l_3}{2}\sin\frac{\theta}{2}}{\cos\alpha}$$

$$s_o = \frac{l_2 + \frac{l_3}{2}\sin\frac{\theta}{2}}{\cos\alpha}$$

Note, the pathlengths s_i and s_o are required to find the proper placements of the dipoles D5I and D5O.

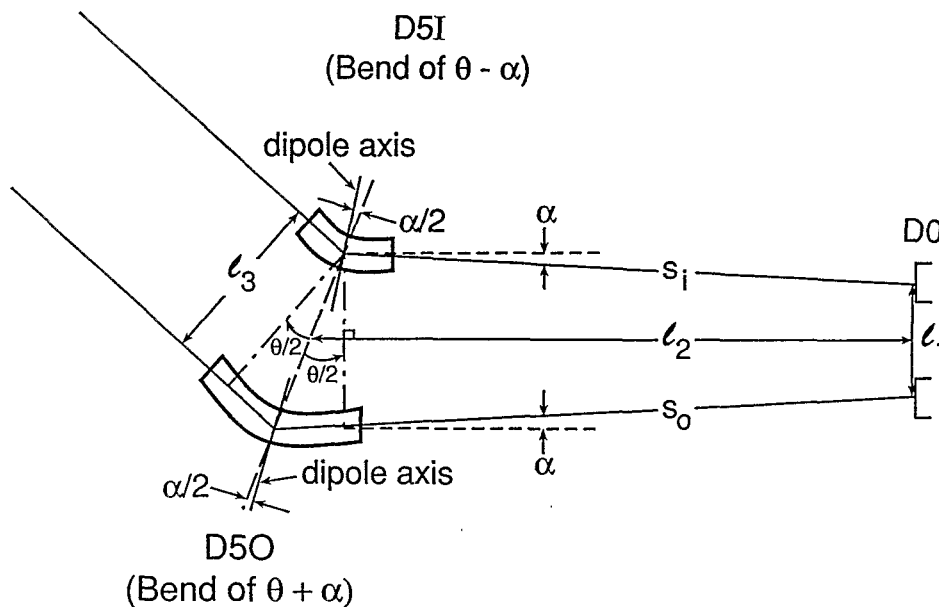


Fig. 26 Geometry of the Dipoles D5I and D5O.